March, 1990] © *1990 The Chemical Society of Japan* *Bull. Chem. Soc. Jpn.*, ***63***, *901—912 (1990)*

Computational Study of the Isomerizations and Fragmentations of the Singlet and Triplet CH_2CH_2NH Diradicals

Takayuki FUENO,* Kizashi YAMAGUCHI, and Osamu KONDO
Department of Chemistry, Faculty of Engineering Science, Osaka University, Toyonaka, Osaka 560

(Received October 18, 1989)

Pathways for the thermal unimolecular reactions of the CH_2CH_2NH diradicals, both singlet and triplet, have been investigated by ab initio MO calculations using 4-31G basis functions. The minimum-energy paths for possible isomerizations and fragmentations are traced by the SCF gradient procedure, and multireference double-excitation (MRD) CI calculations carried out for all the stationary structures located. The results of calculation show that the energetically most favorable unimolecular reaction possible to the triplet diradical is an α-hydrogen detachment giving rise to $CH_2{=}CH{-}NH$ ($^2A''$), whereas that to the singlet diradical is a 1,2-hydrogen migration to give $CH_3CH{=}NH$ ($^1A'$). The activation barrier heights calculated for the two processes are 103 and 74 kJ mol^{-1}, respectively. It is concluded that, in the gas phase, CH_3CN and HCN should be formed concurrently by the α-bond cleavages of the doublet radical $CH_3CH{=}N$ ($^2A'$), which will arise most readily from the vibrationally hot $CH_3CH{=}NH$ ($^1A'$).

Chemistry of the imino radical NH is intriguing in relation to that of atomic oxygen. Despite the close similarity in electronic structure, however, chemical behavior of NH in the gas phase has not yet been explored as comprehensively. Experimental studies worthy of note are only those on the addition of NH toward ethylene,[1] the reactions of NH($X^3\Sigma^-$) with NO and O_2 to give N_2 and NO, respectively,[2,3] the insertion of NH($a^1\Delta$) into a C–H bond of paraffins with a concomitant H atom abstraction,[4,5] and the reaction of NH($a^1\Delta$) with NO giving rise to N_2O ($X^1\Sigma^+$) as the ultimate product.[6] Molecular orbital theoretical studies have greatly assisted understandings of the mechanistic features of chemical reactions of the NH radicals in different electronic states.[6—10]

The reaction of NH($^3\Sigma^-$) with ethylene in the gas phase is one of the most fundamental types of chemical prosseses associated with the NH radical. Cornell, Berry, and Lwowski photolyzed hydrazoic acid HN_3 in the presence of ethylene to investigate the reaction.[1] They found that, under the hot flash and isothermal steady photolysis conditions, the final products were CH_3CN, HCN, CH_4, and H_2. Apparently, the primary step of the reaction is the addition of NH to ethylene:

$$CH_2{=}CH_2 + NH(^3\Sigma^-) \longrightarrow \dot{C}H_2{-}CH_2{-}\dot{N}H \qquad (0)$$

They inferred that the triplet CH_2CH_2NH diradical thus formed would then be isomerized into triplet ethylnitrene CH_3CH_2N, which would subsequently suffer cleavages of the bonds associated with the α-carbon atom, to give CH_3CN and HCN eventually. Although the overall reaction must involve isomerizations (hydrogen atom migrations) and fragmentations (bond scissions), its exact pathway still remains to be clarified. Even the intermediacy of triplet ethylnitrene is a matter of inquiry.

The present study is aimed at unraveling the intricated mechanism of the C_2H_4–NH reaction theoretically. Specifically, the isomerization-fragmentation pathways possible to the CH_2CH_2NH diradicals, both triplet and singlet, are examined by ab initio MO calculations. To this end, the minimum-energy path for each elementary reaction is traced by the SCF procedure to locate the transition state involved. Multireference double-excitation (MRD) configuration-interaction (CI) calculations are then carried out for the transition states as well as the intermediates. It is concluded that the precursor directly responsible for the formations of CH_3CN and HCN sould be a doublet radical $CH_3CH{=}N$ ($^2A'$), which has arisen from the singlet CH_2CH_2NH diradical via the 1,2-hydrogen migration followed by the N–H bond cleavage.

Method of Calculations

Geometries of the CH_2CH_2NH diradicals and their unimolecular reaction intermediates were optimized by the UHF SCF procedure. Those for the stable products in the ground singlet state were treated by the RHF SCF method. The Gaussian 70 program package[11] was used for this purpose. The basis atomic orbital functions adopted were the conventional split-valence 4-31G sets.[12]

The minimum-energy paths for the hydrogen atom migrations and the fragmentation reactions of CH_2CH_2NH were traced mostly by the UHF procedure. Some reactions of the singlet CH_2CH_2NH diradical giving stable ground singlet-state products were treated by a multi-configurational (MC) SCF method. The transition states (energy saddle points) located were checked by the vibrational normal-mode analyses. The necessary force constant matrices were constructed by numerical differentiations of the energy gradients.

All the transition states and the SCF energy minimum structures were then subjected to the MRD-CI calculations.[13] The Table MRD-CI program furnished by Buenker[14,15] was used. The configuration-selection and extrapolation routines[13] were followed. Thus, the minimum threshold T_m for the configuration selection was set equal to a certain value between 5 to 20 μhartrees in order to select 8000—10000 symmetry-adapted configurational functions (SAF) out of the total SAF's generated. For additional threshold values T increasing stepwise from T_m at a 5-μhartree interval were adopted in order to enable the extrapolation of the CI energy to the limit $T \rightarrow 0$. The limiting CI energy thus extrapolated will hereafter be denoted as $E_{CI,T\rightarrow 0}$.

In calculating the CI energies at a given set of T_m and T's, all the configurations whose contributions $|C_i|^2$ to a state under consideration exceed 0.2% were regarded as the reference (main) configurations. The total number of the reference configurations employed was typically 1 to 5 depending on the structure and symmetry of the molecular systems treated, and the total sum of the weights $\sum|C_i|^2$ of the reference configurations usually ranged from 0.90 to 0.95.

The $E_{CI,T\rightarrow 0}$ values tend to be lowered as the numbers of the reference configurations adopted and, hence, their total weights $\sum|C_i|^2$ increase. The uncertainty attached to $E_{CI,T\rightarrow 0}$ is a reflection of insufficiency in the evaluation of the electron correlation effects. The deficiency is remedied by invoking the generalized Langhoff–Davidson correction,[13,16] which is considered to take account of possible correlation errors that may arise from the use of a limited number of reference configurations. The CI energy with this correction can be regarded as an estimate of the full CI limit value.[17,18] Because this corrected CI energy is relatively insensitive to the number of the reference configurations chosen, we will adopt it as the final CI energy throughout this study and will denote it as E_{CI}.

General Outlook

Scheme 1 represents the isomerization and fragmentation pathways possible to the singlet and triplet CH_2CH_2NH diradicals. Various intermediates are arranged in such a manner that in each column the total number of the C, N, and H atoms are retained. On shifting from the first (leftmost) column to the second and the third, the number of the hydrogen atoms bound to the heavy atoms is decreased one by one. Thus, the vertical shifts correspond to isomerizations or the C–C bond scissions, while the shiftings to the right-hand neighboring columns result in hydrogen-atom detachments. The numerical figures appended to the various entries indicate their calculated CI energies E_{CI} plus the energy of the detached hydrogen atom(s), which are expressed in kJ/mol relative to the triplet CH_2CH_2NH diradical. Geometric isomers, cis and trans, are differentiated with the respective subscripts c and t, wherever appropriate. When more than one minimun-energy structure belonging to the same spin state and geometric configuration are found to be possible (as in the staggered vs gauche forms or in the s-cis vs. s-trans conformations), the most stable structure has been selected for listing.

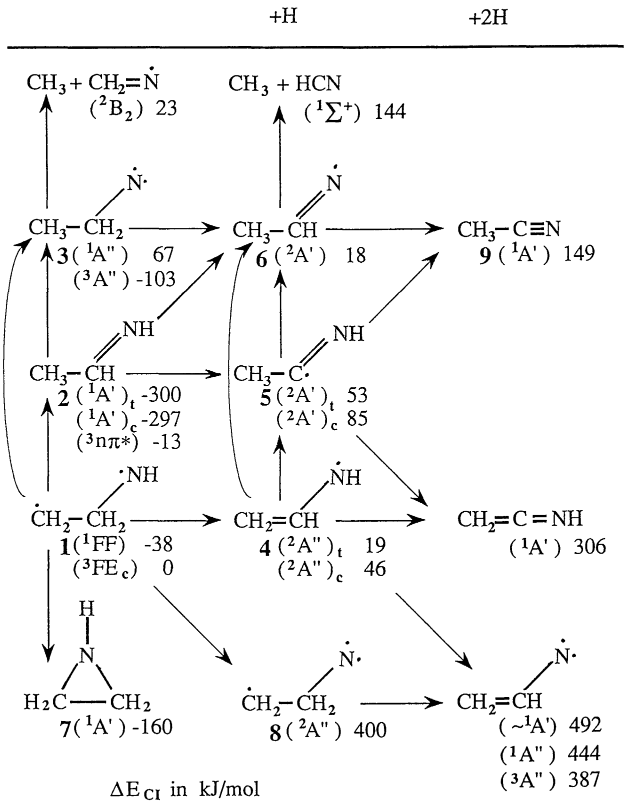

Scheme 1.

Inspection of Scheme 1 shows that the doublet radical which is directly responsible for the formation of CH_3CN is likely to be $CH_3CH=N$ (**6**), the other precursor radical $CH_3C=NH$ (**5**) being less stable and hence being produced with a lesser possibility. HCN will also be formed from **6**. The central issue here is, therefore, how this key radical **6** can be formed from the starting 1,3-diradical CH_2CH_2NH (**1**).

Judging from the stability data calculated for the intermediates alone, the pathway involving an intermediacy of ethanimine $CH_3CH=NH$ (**2**($^1A'$)) appears to be the most favorable in the case of the singlet CH_2CH_2NH. More confidently, however, its possible dominance over the pathways through ethylnitrene (**3**) and the vinylamino radical (**4**) should be judged from the relative heights of the energy barriers involved. Let us denote these pathways leading to the key precursor radical (**6**) as Routes a—c:

Route a $\mathbf{1} \longrightarrow \mathbf{2} \longrightarrow \mathbf{6}$

Route b $\mathbf{1} \longrightarrow \mathbf{3} \longrightarrow \mathbf{6}$

Route c $\mathbf{1} \longrightarrow \mathbf{4} \longrightarrow \mathbf{6}$

Note that the initial steps of Routes a—c are the 1,2-hydrogen migration, 1,3-hydrogen migration, and α-hydrogen elimination, respectively. The relative eases of Routes a—c may well be different in the case of the triplet CH_2CH_2NH.

In what follows, we will exmained the potential energy profiles for Routes a—c theoretically. We will first treat the triplet case, because the species to be formed initially by the addition of $NH(^3\Sigma^-)$ toward ethylene is the CH_2CH_2NH diradical in the triplet state. The case of the singlet CH_2CH_2NH will then be considered likewise. In both cases, whether the second steps giving **6** would indeed be the lowest-energy pathways for **2**, **3**, and **4** will be examined cautiously. Finally, the unimolecular decompositions of **6** will be examined.

Potential Energy Profiles

(A) Reactions of the Triplet CH_2CH_2NH. The CH_2CH_2NH diradical has four stable conformations.[8] These arise from the local geometries of the terminal methylene group in the face (F) and edge (E) orientations to the C–N bond on one hand and from the orientations of the N–H bond s-trans (E_t) and s-cis (E_c) to the C–C bond on the other. Of these four conformations, the most stable is found to be the one in the face-methylene (F) and s-cis (E_c) structure designated as ^3FE_c. In reality, the ^3FE_c conformer has no structural symmetry, though; the dihedral angle $\phi(H^4N^3C^2C^1)$ (see Fig. 1) is 25.8°. Its precise geometry optimized by the UHF SCF procedure is given in

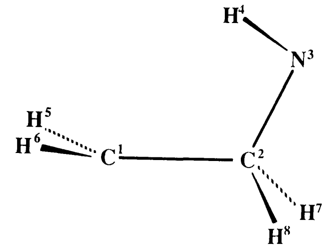

Fig. 1. Labeling of the atoms in the CH_2CH_2NH diradical.

Table 1. Geometry and Energies of the C_2NH_5 Isomers

	Triplet state			Singlet state		
	1	**2**	**3**	**1′**	**2′t**	**3′**[a)]
	(^3FE_c)	($^3n\pi^*$)	($^3A''$)	(^1FF)	($^1A'$)	($^1A'$)
Bond distances (r/Å)						
$r(C^2C^1)$	1.491	1.498	1.531	1.499	1.492	1.531
$r(N^3C^2)$	1.484	1.415	1.462	1.473	1.258	1.447
$r(H^4N^3)$	1.015	1.012		1.015	1.006	
$r(H^4C^1)$			1.082			1.082
$r(H^5C^1)$	1.072	1.087	1.082	1.071	1.085	1.082
$r(H^6C^1)$	1.074	1.084	1.082	1.073	1.079	1.082
$r(H^7C^2)$	1.080	1.075	1.085	1.078	1.083	1.087
$r(H^8C^2)$	1.088		1.085	1.083		1.087
$r(H^8C^1)$		1.082			1.085	
Bond angles (θ/°)						
$\theta(N^3C^2C^1)$	115.6	117.4	111.1	104.5	121.6	112.0
$\theta(H^4N^3C^2)$	110.6	114.8		109.9	115.6	
$\theta(H^4C^1C^2)$			110.8			110.7
$\theta(H^5C^1C^2)$	121.1	111.5	110.8	119.3	110.8	110.7
$\theta(H^6C^1C^2)$	120.5	111.4	110.4	120.1	109.7	110.4
$\theta(H^7C^2C^1)$	111.6	119.2	110.7	111.3	115.9	110.5
$\theta(H^8C^2C^1)$	110.4		110.7	111.6		110.5
$\theta(H^8C^1C^2)$		110.3			110.8	
Dihedral angles (ϕ/°)						
$\phi(H^4N^3C^2C^1)$	25.8	107.2		79.1	180.0	
$\phi(H^4C^1C^2N^3)$			−60.1			−60.0
$\phi(H^5C^1C^2N^3)$	95.1	64.3	60.1	74.8	120.5	60.0
$\phi(H^6C^1C^2N^3)$	−78.0	−55.7	180.0	−86.5	0.0	180.0
$\phi(H^7C^2C^1N^3)$	−121.9	−144.8	−120.4	−116.6	180.0	−120.8
$\phi(H^8C^2C^1N^3)$	119.6	175.7	120.4	122.1		120.8
Energies (E/hartree)						
$E_{SCF}+132$	−0.80058	−0.80610	−0.84971	−0.79917	−0.87181	−0.77798[a)]
$E_{CI,T\to 0}+132$	−1.03306	−1.03944	−1.07094	−1.04633	−1.14207	−1.00527
$E_{CI}+132$	−1.04972	−1.05498	−1.08904	−1.06419	−1.16429	−1.02422

a) Optimized by the two-configurational SCF procedure. It is essentially degenerate with the $^1A''$ state.

Table 1.

We now consider the first steps of Routes a—c:

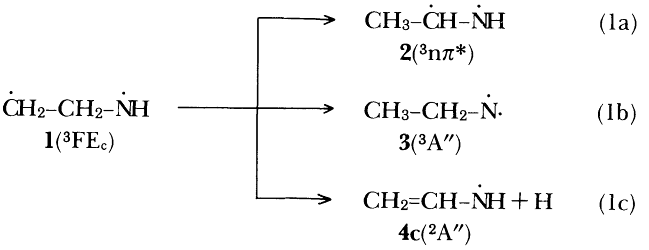

Reaction 1a is a 1,2-hydrogen migration to give ethanimine (**2**) in its first excited triplet state (^{3}nπ*). Reaction 1b is a 1,3-hydrogen migration giving triplet ethylnitrene (**3**(^{3}A″)). The radical formed by reaction 1c is the cis isomer of the vinylamino radical (**4**) in its ground electronic state (^{2}A″). The optimized geometries of the products **2** and **3** are given in Table 1. The geometry optimized for the doublet radical **4c**(^{2}A″) is given in Table 2.

The minimum-enegry paths for the unimolecular reactions 1a—c have been traced by the SCF calculations. Geometries of the respective transition states TS1(a)—(c) located are illustrated in Fig. 2. Only the TS1(b) is symmetric (C_s) with respect to the CCN skeletal plane.

MRD-CI calculations have been carried out for the reactant (**1**), products (**2**—**4**), and the transition states. The activation barrier heigths $\Delta E_{\mathrm{CI}}^{\neq}$ and the energy changes for reaction ΔE_{CI} have then been evaluated

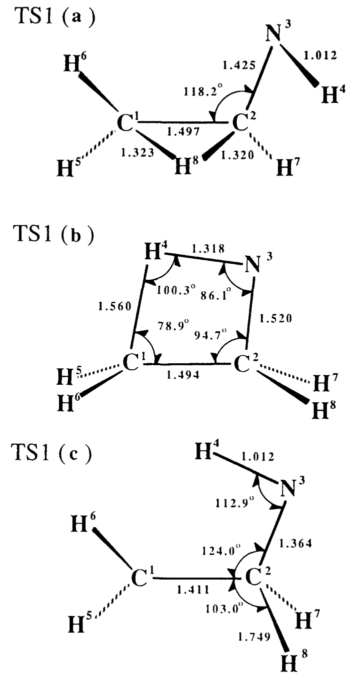

Fig. 2. Transition state geometries for unimolecular reactions of **1** (^{3}FE$_c$). Bond distances are given in units of Å. TS1(a), reaction 1a; TS1(b), reaction 1b; TS1(c), reaction 1c.

Table 2. Geometry and Energies of the C_2NH_4 Isomers

	4c (^{2}A″)	**4t** (^{2}A″)	**5c** (^{2}A′)	**5t** (^{2}A′)	**6** (^{2}A′)
Bond distances (r/Å)					
$r(C^2C^1)$	1.389	1.386	1.487	1.484	1.504
$r(N^3C^2)$	1.335	1.334	1.243	1.244	1.280
$r(H^4N^3)$	1.011	1.008	1.014	1.005	
$r(H^4C^1)$					1.080
$r(H^5C^1)$	1.073	1.071	1.082	1.082	1.083
$r(H^6C^1)$	1.071	1.071	1.082	1.082	1.083
$r(H^7C^2)$	1.074	1.078	1.086	1.083	1.079
Bond angles (θ/°)					
$\theta(N^3C^2C^1)$	126.1	120.5	137.4	130.7	123.6
$\theta(H^4N^3C^2)$	113.6	113.8	120.5	119.0	
$\theta(H^4C^1C^2)$					110.9
$\theta(H^5C^1C^2)$	121.4	119.7	110.2	110.4	110.4
$\theta(H^6C^1C^2)$	121.1	121.5	110.2	110.4	110.4
$\theta(H^7C^2C^1)$	118.8	118.5	111.7	110.4	118.1
Dihedral angles (ϕ/°)					
$\phi(H^4N^3C^2C^1)$	0.0	180.0	0.0	180.0	
$\phi(H^4C^1C^2N^3)$					0.0
$\phi(H^5C^1C^2N^3)$	0.0	0.0	120.7	120.6	120.5
$\phi(H^6C^1C^2N^3)$	180.0	180.0	−120.7	−120.6	−120.5
$\phi(H^7C^2C^1N^3)$	180.0	180.0	0.0	0.0	180.0
Energies (E/hartree)					
$E_{\mathrm{SCF}}+132$	−0.26873	−0.26950	−0.23993	−0.24627	−0.28015
$E_{\mathrm{CI,T}\to 0}+132$	−0.51672	−0.52633	−0.49934	−0.51188	−0.52531
$E_{\mathrm{CI}}+132$	−0.53401	−0.54421	−0.51894	−0.53125	−0.54464

Table 3. Activation Barrier Heights and the Energy Changes for Unimolecular Reactions of the CH_2CH_2NH Diradicals (kJ mol^{-1})[a)]

No.	Reaction	Spin multiplicity	Barrier heights		Energy changes	
			$\Delta E_{CI}^{\ddagger}$	$\Delta E_0^{\ddagger}$ b)	ΔE_{CI}	ΔE_0 b)
0	$C_2H_4+O(^3P)\rightarrow$ **1**	3	49	56	−1	11
1a	**1**→**2**	3	228	219	−13	−8
1b	**1**→**3**	3	117	108	−103	−92
1c	**1**→**4c**+H	3	103	86	46	23
1d	**1**→$CH_2+CH_2{=}NH$	3	131	121	109	94
1′a	**1′**→**2′t**	1	74	73	−263	−248
1′b	**1′**→**3′**	1	226	213	105	113
1′c	**1′**→**4t**+H	1	172	152	57	31
2a	**2**→**3**	3	164	143	−90	−84
2b	**2**→**5c**+H	3	135	104	99	69
2c	**2**→**6**+H	3	115	93	32	3
2′a	**2′t**→**3′**	1	380	359	368	361
2′b	**2′t** →**5t**+H	1	No barrier top		354	313
2′c	**2′t**→**6**+H	1	No barrier top		319	277
2′d	**2′t**→$CH_3+CH{=}NH$	1	No barrier top		388	347
3a	**3**→**6**+H	3	169	140	121	86
3b	**3**→$CH_3+CH_2{=}N$	3	140	118	126	90
3′a	**3′**→**6**+H	1	55	29	−49	−84
3′b	**3′**→$CH_3+CH_2{=}N$	1	46	24	−44	−80
3′c	**3′**→**2′t**	1	12	0	−368	−361
4a	**4c**→**5c**	2	292	271	39	38
4b	**4c**→**6**	2	169	148	−28	−29
4′a	**4t**→**5t**	2	320	299	34	33
4′b	**4t**→**6**	2	196	174	−1	−2
5a	**5c**→**6**	2	221		−35	−31
5b	**5c**→CH_3CN+H	2	105		63	39
6a	**6**→CH_3CN+H	2	156	133	131	106
6b	**6**→CH_3+HCN	2	147	128	126	102

a) Calculated using the 4-31G basis sets.[12)] b) Corrected for the vibrational zero-point energies; the subscript 0 stands for CI+vib.

from these CI energy data. Both the $\Delta E_{CI}^{\ddagger}$ and ΔE_{CI} values are corrected for the vibrational zero-point energy and denoted as $\Delta E_0^{\ddagger}$ and ΔE_0, respectively. All the results are collected in Table 3.

As can be seen in Table 3, reaction 1c has the lowest energy barrier $\Delta E^{\ddagger}$, even though its product state has the highest ΔE and hence is the least stable. The CI energy barrier $\Delta E_{CI}^{\ddagger}$ calculated for reaction 1c is 103 kJ mol^{-1}. It is noteworthy that the $\Delta E_{CI}^{\ddagger}$ value (117 kJ mol^{-1}) for the 1,3-hydrogen migration (1b) is much lower than that (228 kJ mol^{-1}) for the 1,2-hydrogen migration (1a), so that reaction 1b may well compete with reaction 1c. The barrier heights $\Delta E_0^{\ddagger}$ for reactions 1b and 1c corrected for the vibrational zero-point energy are 108 and 86 kJ mol^{-1}, respectively.[19)]

We next examine the second steps of Routes a—c, i. e., the unimolecular processes of **2**, **3**, and **4c**. For the triplet intermadiate **2**($^3n\pi^*$), possible candidates are:

$$\mathbf{2}(^3n\pi^*) \longrightarrow \mathbf{3}(^3A'') \qquad (2a)$$

$$\mathbf{2}(^3n\pi^*) \longrightarrow \mathbf{5c}(^2A') + H \qquad (2b)$$

$$\mathbf{2}(^3n\pi^*) \longrightarrow \mathbf{6}(^2A') + H \qquad (2c)$$

Reaction 2a is the 1,2-hydrogen migration from the nitrogen atom onto the α-carbon atom. Reactions 2b and 2c are hydrogen atom detachments from the α-carbon and the nitrogen atoms, respectively.

Geometries of the product doublets **5c** and **6** and those for the transition states of reactions 2a—c were optimized by the SCF procedure. The geometrical parameters obtained for **5c** and **6** are given in Table 2.

MRD-CI calculations were then carried out for the three transition states. The activation barrier heights $\Delta E^{\ddagger}$ evaluated are given in Table 3. The barrier heights based on the E_{CI} data are 164, 135, and 115 kJ mol^{-1}, for reactions 2a, 2b, and 2c, respectively. Apparently, reaction 2c giving rise to **6** is the most favorable of the three elementary reactions under consideration. The TS geometry (TS2) of this particular reaction is illustrated in Fig. 3.

The second step of Route b is

$$\mathbf{3}(^3A'') \longrightarrow \mathbf{6}(^2A') + H \qquad (3a)$$

The TS geometry obtained is illustrated in Fig. 3 (TS3). The barrier height calculated by the CI procedure is $\Delta E_{CI}^{\ddagger}$=169 kJ mol^{-1}. Whether reaction 3a will indeed be the most favorable pathway for the

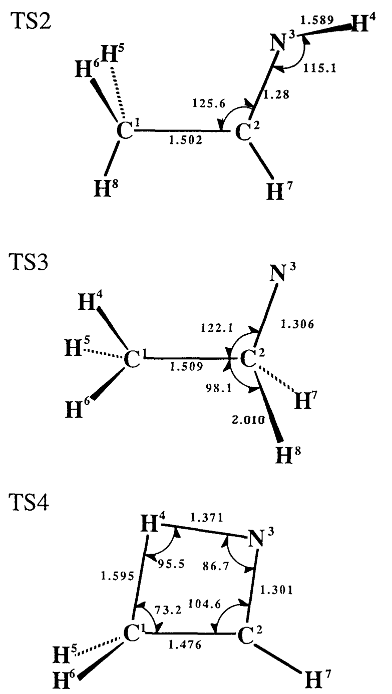

Fig. 3. Transition state geometries for the reactions giving **6** ($^2A'$). Bond distances are given in units of Å. TS2, reaction 2c; TS3, reaction 3a; TS4, reaction 4b.

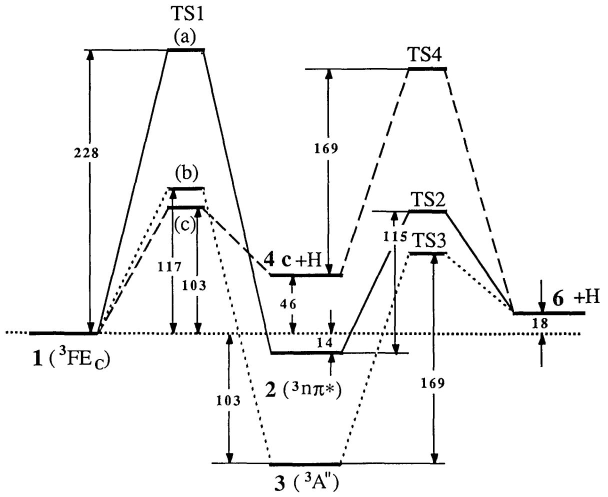

Fig. 4. Potential energy profiles for the reactions of triplet CH_2CH_2NH (^3FE_c) leading to the formation of $CH_3CH{=}N$ (**6**). The energy gaps shown (kJ mol^{-1}) are based on the calculated E_{CI} values. —, Route a (reaction 1a followed by reaction 2c); ······, Route b (reaction 1b followed by reaction 3a); – – –, Route c (reaction 1c followed by reaction 4b).

unimolecular decomposition of **3**($^3A''$) needs to be judged cautiously, however.[20]

The transition states for the 1,2- and 1,3-hydrogen migrations of **4c** ($^2A''$)

$$4c(^2A'') \longrightarrow 5c(^2A') \qquad (4a)$$

$$\qquad\quad \longrightarrow \mathbf{6}(^2A') \qquad (4b)$$

were examined likewise. CI treatments have given the barrier heights $\Delta E_{CI}^{\neq}$ of 292 and 169 kJ mol^{-1} for reactions 4a and 4b, respectively. The 1,3-hydrogen migration (4b) is far more favorable than the 1,2-hydrogen migration (4a) just as in the case of the triplet diradical **1**. Since the hydrogen detachments giving ketimine and vinylnitrene are both highly endothermic, it is doubtless that reaction 4b giving **6**($^2A'$) is the most favorable process possible to **4c**($^2A''$). The TS geometry (TS4) for reaction 4b as the second step of Route c is illustrated in Fig. 3.

5c($^2A'$) is a relatively unstable species. Of its two decompositions:

$$5c(^2A') \longrightarrow \mathbf{6} \qquad (5a)$$

$$\qquad\quad \longrightarrow CH_3CN + H \qquad (5b)$$
$$\mathbf{9}(^1A')$$

reaction 5b should be kinetically the more dominant, the calculated $\Delta E_{CI}^{\neq}$ being 220 and 105 kJ mol^{-1} for reactions 5a and 5b, respectively. Either way, however, the formation of **5c** itself is difficult, as has already been described. Therefore, any mechanism involving the intermediacy of **5** can totally be ignored.

In Fig. 4, the potential energy profiles for Routes a—c of our concern obtained on the basis of the E_{CI} values are compared. Although the first step (reaction 1c) of Route c is energetically the most favorable, its second step (reaction 4b) is a process of a considerably high activation energy barrier. The first step of Route b (reaction 1b) giving triplet ethylnitrene (**3**) is perhaps capable of competing with reaction 1c. However, because the transition state of its second step (reaction 3a) lies below the barrier top of the first step, the triplet nitrene, if formed by the first step, will get decomposed spontaneously. There is no doubt that Route a is the least favorable pathway for **1** to lead to **6**.

(B) Reaction of the Singlet CH_2CH_2NH. According to Cvetanović, the reaction of the O(^3P) atom with ethylene in the gas phase gives ethylene oxide and acetaldehyde as the principal products.[21] He has concluded that the triplet CH_2CH_2O diradical formed initially by the addition of O(^3P) toward ethylene converts itself into a singlet state, which in turn undergoes the ring-closure and the 1,2-hydrogen migration. By analogy to this scheme, the triplet CH_2CH_2NH diradical upon its formation by reaction 0 may suffer an intersystem crossing into the singlet state before undergoing the isomerization and fragmentation reactions. Examinations of the potential energy profiles for the singlet-state counterparts of Routes a—c thus appear to be indispensable in this context.

In the case of the singlet CH_2CH_2NH diradical (**1′**) also, there can exist four equilibrium conformations.[8] As in the case of triplet CH_2CH_2NH, the terminal CH_2 group can be in either the face (F) or the edge (E) orientation. The N–H bond, on the other hand, either lies in the s-trans orientation (E_t) with the dihedral angle $\phi(H^4N^3C^2C^1)=180°$ or is projected out of the CCN skeletal plane in the face form (F), for which $\phi(H^4N^3C^2C^1)=79.1°$. Of the four conformations arising from the combinations of the local geometries of the CH_2 group and the N–H bonding, the most stable is the one that has both the CH_2 and NH group in the face form, which is designated as ^1FF.[8] Detailed geometrical parameters of CH_2CH_2NH (^1FF) are given in the fourth column of Table 1.

The ^1FF conformer is structurally unique in that its two singly-occupied molecular orbitals (SOMO) localized mostly on the terminal C and N atoms lie nearly on the plane of the CCN skeleton. This implies a bonding interaction between the SOMO's to effect a special stabilization of this conformer. In fact, MRD-CI calculations have shown that ^1FF is more stable by 38 kJ mol^{-1} than ^3FE_c, and its diradical character is diminished appreciably. The bonding interaction develops continuously as the CCN bond angle is decreased. Thus, ^1FF cyclizes into aziridine (**7**) with virtually no activation barrier, a process which constitutes the most favorable pathway of isomerization possible to the singlet CH_2CH_2NH. Variations in electronic structure with the progress of cyclization was described in detail in a previous paper.[8]

The issues which we concern primarily in the present study are the energetics for the isomerization-fragmentation Routes a—c. As in the case of the triplet diradical (^3FE_c), the first steps of these routes are represented as follows:[22]

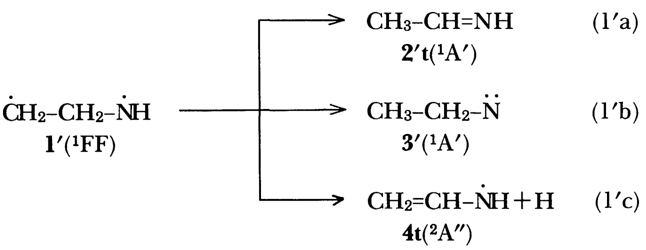

In tracing the minimum-energy path for reaction 1′a, the multi-configurational (MC) SCF method has been used, since a considerable extent of closed-shell character has proved to inhere in its transition state. Specifically, a six-electron five-orbital model was adopted for use. For reactions 1′b and 1′c, the UHF SCF procedure was utilized for the sake of expedience.[23] The TS geometries obtained, TS1′(a)—(c), are shown in Fig. 5. As in the case of the triplet diradical, only TS1′(b) for the 1,3-hydrogen migration (reaction 1′b) takes on a symmetric (C_s) structure. Geometry parameters for the singlet products **2′**t($^1A'$) and **3′**($^1A'$) are given in Table 1. Geometry of the doublet product **4**t($^2A''$) is listed in Table 2.

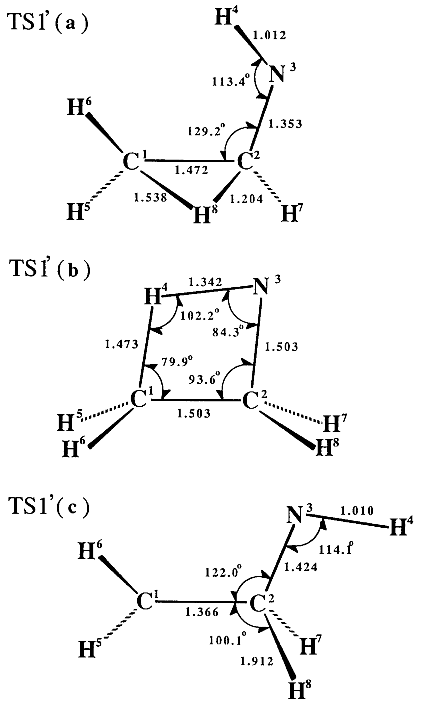

Fig. 5. Transition state geometries for unimolecular reactions of **1′** (^1FF). Bond distances are given in units of Å. TS1′(a), reaction 1′a; TS1′(b), reaction 1′b; TS1′(c), reaction 1′c.

All the products and the transition states have then been subjected to MRD-CI calculations. The activation barrier heights $\Delta E_{CI}^{\neq}$ and the energy changes for reaction ΔE_{CI} were evaluated from the CI energy values obtained. The results are given in Table 3, together with the $\Delta E_0^{\neq}$ and ΔE_0 values.

As the CI energy data listed in Table 3 show, the barrier height for the 1,2-hydrogen migration (reaction 1′a) is markedly low in the case of the singlet CH_2CH_2NH diradical, the $\Delta E_{CI}^{\neq}$ value being 74 kJ mol^{-1}. Neither reaction 1′b, for which $\Delta E_{CI}^{\neq}=226$ kJ mol^{-1}, nor reaction 1′c, for which $\Delta E_{CI}^{\neq}=172$ kJ mol^{-1}, can possibly compete with reaction 1′a. Reaction 1′a is also far more preferential over the various unimolecular reactions of the triplet diradical. Its activation barrier height corrected for the vibrational zero-point energy is $\Delta E_0^{\neq}=73$ kJ mol^{-1}.

The second step of Routes a—c are:

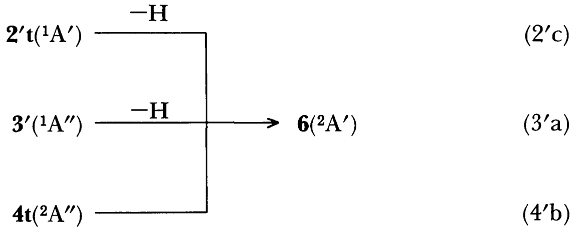

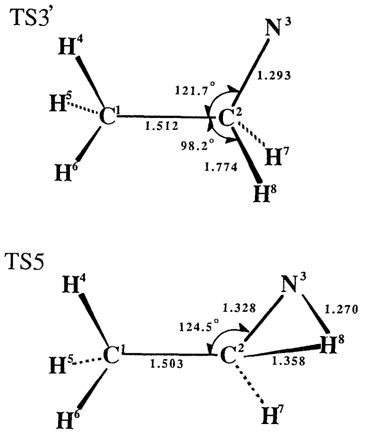

Fig. 6. Transition state geometries for unimolecular reactions of singlet $CH_3CH_2N(\mathbf{3'})$. Bond distances are given in units of Å. TS3', reaction 3'a; TS5, reaction 3'c.

Obviously, there is no energy barrier in reaction 2'c; the endothermicity arising from the N–H bond cleavage should constitute an essential part of its activation energy.[24] The TS for reaction 4'b should be common to that for reaction 4b, since **4t** has first to take the cis form in order to enter into the 1,3-hydrogen transfer. The TS geometry for reaction 3'a (TS3') is shown in Fig. 6. It is essentially similar to that for its triplet counterpart, reaction 3a, although it lies at a somewhat earlier stage of reaction, the C^2–H^8 bond distances at the transition staes being 1.774 and 2.010 Å for reactions 3'a and 3a, respecively.

MRD-CI calculation was required only for reaction 3'a. Unlike the case of triplet ethylnitrene ($^3A''$), the α-hydrogen detachment from singlet ethylnitrene ($^1A''$) has a relatively low activation barrier height. Its $\Delta E_{CI}^{\ddagger}$ value is as low as 55 kJ mol^{-1}, while that for the triplet nitrene is 169 kJ mol^{-1} (see Table 3).[25]

Figure 7 illustrates the E_{CI}-based potential energy profiles of Routes a—c for the case of the singlet CH_3CH_2NH diradical. Evidently, Route a via an intermediacy of ethanimine $CH_3CH=NH$ (**2**) in its ground electronic state is the most favorable pathway to $CH_3CH=N$ (**6**) in the singlet potential-energy space. It is also more advantageous than any reaction path possible on the triplet energy surfaces.

(C) Decompositions of $CH_3CH=N$. The doublet radical (**6**) is thought to be an immediate precursor to CH_3CN and HCN, which are the ultimate products of the ethylene–NH reaction. CH_3CN and HCN are to be formed by the α-hydrogen detachment and the C–C bond cleavage, respectively:

$$\mathbf{6}(^2A') \longrightarrow CH_3CN + H \qquad (6a)$$

$$\phantom{\mathbf{6}(^2A')} \longrightarrow CH_3 + HCN \qquad (6b)$$

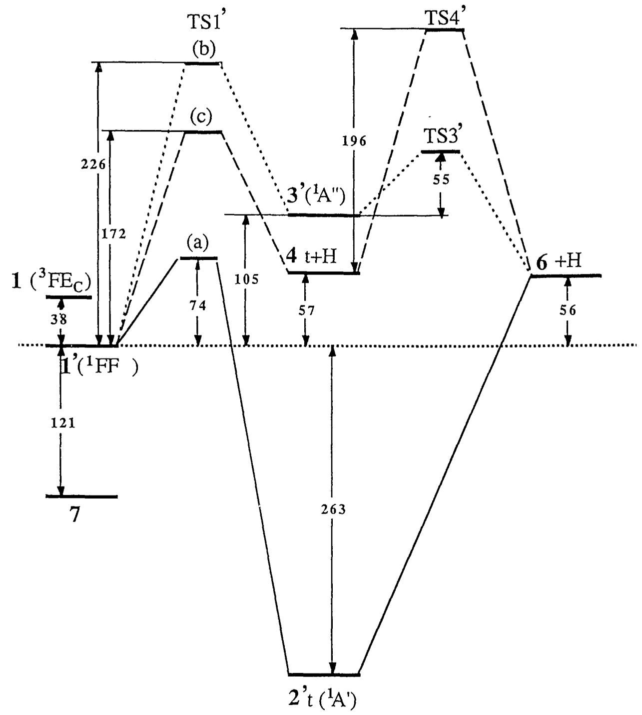

Fig. 7. Potential energy profiles for the reactions of singlet CH_2CH_2NH (^1FF) leading to the formation of $CH_3CH=N$ (**6**). The energy gaps shown (kJ mol^{-1}) are based on the calculated E_{CI} values. —, Route a (reaction 1'a followed by reaction 2'c); ······, Route b (reaction 1'b followed by reaction 3'a); ———, Route c (reaction 1'c followed by reaction 4'b).

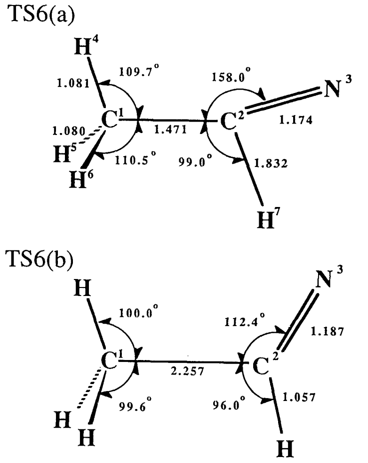

Fig. 8. Transition state geometries for the decomposition of $CH^3CH=N$ (**6**). TS6(a) reaction 6a; TS6(b), reaction 6b.

It is confirmed by SCF calculations that both decompositions proceed by maintaining the C_s-symmetry. Geometries for the transition states TS6(a) and (b) located are shown in Fig. 8.

Results of subsequent MRD-CI calculations for reactions 6a and 6b are compared in Table 3. Reaction 6a appears to be slightly less favorable than reaction

6b; the CI barrier height $\Delta E_{CI}^{\neq}$ for the former reaction is 156 kJ mol^{-1}, while that for the latter is 147 kJ mol^{-1}. Vibrational energy corrections have lowered the barrier heights to 133 and 128 kJ mol^{-1}, respectively, as is shown in Table 3. Relative dominances of reactions 6a and 6b are thus hard to predict. The branching ratio will be nearly half and half with a marginal preference of the latter reaction (6b) over the former (6a).

Discussion

As can be seen in Scheme 1, the ethaniminyl radical $CH_3CH=N$ (**6**) is the most stable entity of the various C_2NH_4 doublets. It is also regarded as a key intermediate in the C_2H_4–NH reaction system in the sense that it can be a direct precursor radical for the formations of CH_3CN and HCN as ultimate stable products.

According to the potential energy profiles calculated in the present work (Figs. 4 and 7), the energetically most favorable pathway leading to the formation of **6** is Route a over the *singlet* potential energy surface. The pathway involves the intermediacy of the ground-state ethanimine $CH_3CH=NH$ (**2′**), which should result readily from the 1,2-hydrogen migration of the singlet CH_2CH_2NH diradical (^{1}FF). The imine **2′**(^{1}A′) upon its formation by the hydrogen migration is energetically hot, i.e., vibrationally energized sufficiently highly to effect the N–H bond scission to give **6**.

As has already been mentioned, the most favorable pattern of isomerization possible to CH_2CH_2NH (^{1}FF) is its cyclization giving aziridine (**7**)

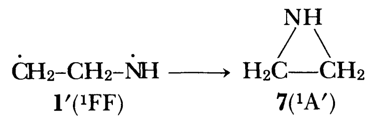

1′(^{1}FF) **7**(^{1}A′) (7)

The product aziridine should, however, be vibrationally hot at the instance of its formation in the gas phase. In other words, **7** should remain in dynamical equilibrium with **1′** (^{1}FF) unless its excess internal energy is removed efficiently. In fact, there is no indication that aziridine is found in the product mixture of the C_2H_4–NH reaction in the gas phase.[1] The singlet CH_2CH_2NH diradical (^{1}FF) may well suffer the hydrogen migration and detachment to give **6** before the hot cyclic isomer (**7**) is vibrationally deactivated.

The above arguments are based on the presumption that the diradical formed by the addition of NH($^3\Sigma^-$) toward ethylene has been converted into the singlet state before it enters into subsequent isomerizations and fragmentations. If the spin conversion is not efficient, the CH_2CH_2NH diradical (^{3}FF$_c$) will be most liable to give the vinylamino radical **4c** (^{2}A″) according to reaction 1c, for which $\Delta E_{CI}^{\neq}$=103 kJ mol^{-1}. The doublet species **4** seems to be a fairly stable radical; it is reluctant to fragmentations (see Shceme 1). Its most favorable unimolecular reaction is the 1,3-hydrogen migration to give **6**, the calculated barrier height being 169 kJ mol^{-1}. Attempts to identify **4** spectroscopically are worthwhile in order to clarify whether or not the C_2H_4–NH reaction can proceed over the triplet-state potential energy surfaces.

The second possibility of the unimolecular reaction of the triplet diradical (^{3}FE$_c$) is the 1,3-hydrogen migration (1b) giving *triplet* ethylnitrene **3**(^{3}A″). Reaction 1b could well compete with the α-hydrogen detachment (1c); the activation barrier height calculated for the former reaction is 117 kJ mol^{-1}, which is only a bit greater than the value 103 kJ mol^{-1} calculated for the latter. The triplet nitrene, if it is formed, will be collapsed into **6** spotaneously, as can be understood from Fig. 4. Thus, Route b of the triplet reaction involving an intermediacy of **3**(^{3}A″) appears at first sight to be an unignorable possibility to the occurrence of the key radical **6**. However, there is one strong drawback against this possibility. That is, **3**(^{3}A″) is more susceptible to the C–C bond cleavage (3b) than to the α-hydrogen detachment (3a); the activation barrier heights calculated for these two reactions are 140 and 169 kJ mol^{-1}, respectively, which are lowered to 118 and 140 kJ mol^{-1}, respectively, by the vibrational zero-point energy corrections. The view that CH_3CN will be formed through an intermediacy of triplet ethylnitrene[1] is, therefore, somewhat dubious.

Investigations of the unimolecular reactions of ethylnitrene are most relevant to the above issue. Cornell et al.[1] photolyzed ethyl azide $C_2H_5N_3$ in the gas phase for this purpose. They found that the main gaseous products were CH_3CN and HCN also in this case in the product ratio being approximately the same as that observed in the C_2H_4–NH reaction. The results suggest strongly that the two types of reactions, i.e., the $C_2H_5N_3$ photolysis and the C_2H_4–NH reaction, proceed via a common intermediate which is capable of giving rise to CH_3CN and HCN. Cornell et al. took this finding as an indication that both the reactions involved the intermediacy of triplet ethylnitrene. Logically, however, the common intermediate mentioned above need not be ethylnitrene, if the nitrene generated by the azide photolysis readily suffers hydrogen detachment to give **6**. In other words, it may well be **6** itself that should be regarded as the common intermediate. The result of the ethyl azide photolysis, therefore, cannot be evidence against the possibility that **6** is formed most favorably through ethanimine (^{1}A′) in the case of the C_2H_4–NH reaction.

Recently, Bock and Dammel[27] have developed extensive investigations of the pyrolysis of azides in the gas phase. According to their observations, the ultimate products of pyrolysis in the case of alkyl azides are nitriles almost exclusively. More important in relation to the present context is their revelation that the singlet imines RCH=NH as the intermediates of pyrolysis are identifiable by the photoelectron spectroscopy or can actually be isolated in some cases. They infer that the alkyl azides are decomposed thermally to give *singlet* imines either directly (by a concerted 1,2-hydrogen migration with the N–N_2 bond cleavage) or by an intermediacy of *singlet* alkylnitrenes. Our calculation shows that singlet ethylnitrene (**3′**) can readily isomerize into trans-ethanimine (**2′t**($^1A'$)) by a hydrogen atom migration from the α-carbon onto the nitrogen atom (reaction 3′c)[25]; the calculated barrier height is as low as $\Delta E_{CI}^{\neq}=12$ kJ mol^{-1}. The imine **2′t** thus formed should be "chemically activated" to enter into the N–H bond cleavage almost spontaneously to give **6**. The processes **3′**→**2′t**→**6**, i. e., reaction 3′c (TS5) followed by reaction 2′c, must be the most dominant unimolecular reaction route for singlet ethylnitrene (**3′**).

The overall mechanism of the C_2H_4–NH reaction has a close similarity to the mechanistic pattern of the reaction between ethylene and the triplet oxygen(^3P) atom. Beside Cvetanović's demonstrations,[21] which have already been mentioned, the following two channels of the reaction have recently been disclosed experimentally:

$$CH_2{=}CH_2 + O(^3P) \longrightarrow CH_3 + CHO \tag{8a}$$
$$\longrightarrow CH_2CH{=}O + H \tag{8b}$$

The concurrent formations of the formyl radical CHO and the formylmethyl radical $CH_2CH{=}O$ have been observed by the ultraviolet absorption spectroscopy[28] and by the microwave kinetic spectroscopy.[29] In either channel of reaction, the initial step must be the addition of O(^3P) toward ethylene to give the CH_2CH_2O diradical. Apparently, reaction 8a is a consequence of the C–C bond cleavage of the vibrationally hot acetaldehyde which has resulted from the 1,2-hydrogen migration of the CH_2CH_2O diradical. Reaction 8b, on the other hand, is due to the α-hydrogen elimination of the diradical. Theoretical investigations[30] show that the 1,2-hydrogen migration of *singlet* CH_2CH_2O diradical to give CH_3CHO is an elementary reaction having a noticeably low energy barrier, while the most favorable unimolecular reaction of the *triplet* CH_2CH_2O diradical is the α-hydrogen detachment. The results of the theoretical studies are not only in harmony with the experimental findings but also in line with the conclusions reached for the case of the CH_2CH_2NH radical of our present concern.

The major mechanistic difference of the CH_2CH_2-NH case from the isoelectronic CH_2CH_2O case lies in the fact that the ground-state $CH_3CH{=}NH$ formed from the singlet CH_2CH_2NH diradical is more subject to the N–H bond scission (reaction 2′c) than to the C–C bond cleavage (reaction 2′d). Chemical behavior of the doublet radical (**6**) should constitute an important final step of the C_2H_4–NH reaction in the gas phase. The ease of this final step hinges on the height of its activation barrier. The step is essentially unimolecular decompositions to give CH_3CN and HCN, i.e., reactions 6a and 6b. The calculated barrier heights for reactions 6a and 6b are 156 and 147 kJ mol^{-1}, respectively. When vibrational zero-point energy corrections are made, these are reduced respectively to the theoretical activation energies $\Delta E_0^{\neq}=133$ and 128 kJ mol^{-1}. The results indicate that reactions 6a and 6b can proceed competitively with each other to give nearly equal amounts of CH_3CN and HCN under different conditions, in harmony with the experimental results.[1,26]

On all these grounds, the most probable pathway for the reaction between ethylene and NH is likely to be the one which involves the intermediacy of $CH_3CH{=}NH$ (**2′t**($^1A''$)) followed by $CH_3CH{=}N$ (**6**($^2A'$)). The triplet CH_2CH_2NH diradical (**1**(^3FE_c)), which might be formed by the addition of NH($^3\Sigma^-$) toward ethylene, would be spin-converted into the singlet state to give **1′**(^1FF). Because the addition of NH($^3\Sigma^-$) toward C_2H_4, reaction 0, is calculated to be nearly thermoneutral and because its calculated barrier height is 49 kJ mol^{-1},[8] the adduct will possess an internal energy sufficient to overcome the barrier for the process **1′**→**2′t** to reach **6**+H eventually (see Fig. 7). The doublet radical **6** will then be decomposed thermally to give CH_3CN and HCN in nearly equal amounts.

Finally, it will be most appropriate to make comments on the accuracy of the present theoretical computations. In this work, all calculations have been based on the conventional 4-31G basis sets throughout. Generally, however, results of such calculations are dependent on the size of the basis functions used, particularly on the use of polarization functions. In order to check these points, we calculated the energy changes ΔE for the overall reactions

$$CH_2{=}CH_2 + NH(^3\Sigma^-) \longrightarrow CH_3CN + 2H \tag{9a}$$
$$\longrightarrow CH_3 + HCN + H \tag{9b}$$

using the 6-31G** basis sets[31] as well as the 4-31G functions. The reason for choosing these reactions is simply that the experimental heat-of-formation data are available for all the species involved.[32,33] The results of calculation are summarized in Table 4.

As can be seen in Table 4, the ΔE_0 values calculated using the 4-31G sets are in reasonably good agreement with the experimental heats of reaction ΔH°. With the 6-31G** sets, the relative stabilities of the product

Table 4. Comparisons of the Calculated Energy Changes (ΔE) for the Overall Reactions 9a and 9b with the Experimental Heats of Reaction (ΔH°)

Reaction	Basis set[a]	ΔE/kJ mol^{-1}			ΔH°[c]
		SCF	CI	CI+vib[b]	kJ mol^{-1}
9a	4-31G//4-31G	216	148	112	112±12
	6-31G**//6-31G**	190	128	91	
9b	4-31G//4-31G	189	143	102	92±12
	6-31G**//6-31G**	165	112	76	

a) The basis sets used for the MRD-CI calculations // the sets used for the SCF geometry optimizations. b) ΔE_0, corrected for the vibrational zero-point energies. c) Based on the heat-of-formation data available in the literature.[32,33]

states (CH_3CN+2H being ca. 20 kJ mol^{-1} less stable than $CH_3+HCN+H$) are better reproduced, but the absolute values for ΔE_0 show no better agreement with ΔH° than do the 4-31G results. Probably, the results of the 4-31G CI calculations given in this work are mostly accurate to within 10 kJ mol^{-1}, so that they will be sufficiently reliable for at least semiquantitative considerations of the energetics of the various elementary processes involved.

Conclusion

1. The doublet radical $CH_3CH{=}N(^2A')$, which must be the direct precursor to CH_3CN and HCN, will arise most readily from the vibrationally hot ethanimine $CH_3CH{=}NH(^1A')$.

2. Ethanimine is formed from the singlet CH_2CH_2NH diradical by the 1,2-hydrogen atom migration, the barrier height being 74 kJ mol^{-1}.

3. The most favorable reaction pathway possible to the triplet CH_2CH_2NH is the α-hydrogen detachment giving the vinylamino radical $CH_2{=}CHNH(^2A')$, the calculated barrier height being 103 kJ mol^{-1}.

4. Singlet ethylnitrene CH_3CH_2N, if formed chemically in the gas phase, will readily be isomerized into ethanimine; the calculated barrier height for the isomerization is as low as 12 kJ mol^{-1}.

This work was supported by the Grants-in-Aid Nos. 61470007 and 62303002 from the Ministry of Education, Japan. The authors are grateful to Professor R. J. Buenker for supplying his Table MRD-CI program to them. All calculations were carried out on a HITAC M-280 at the Computer Center of the Institute for Molecular Science. The authors thank the Center for an allocation of CPU time.

References

1) D. W. Cornell, R. S. Berry, and W. Lwowski, *J. Am. Chem. Soc.*, **88**, 544 (1966).

2) I. Hansen, K. Hoingehaus, C. Zetzsch, and F. Stuhl, *Chem. Phys. Lett.*, **42**, 370 (1976).

3) C. Zetzsch and I. Hansen, *Ber. Bunsen-Ges. Phys. Chem.*, **82**, 830 (1978).

4) O. Kajimoto and T. Fueno, *Chem. Phys. Lett.*, **80**, 484 (1981).

5) O. Kondo, J. Miyata, O. Kajimoto and T. Fueno, *Chem. Phys. Lett.*, **88**, 424 (1982).

6) T. Fueno, M. Fukuda, and K. Yokoyama, *Chem. Phys.*, **124**, 265 (1988).

7) W. J. Haines and I. G. Csizmadia, *Theor. Chim. Acta (Berl.)*, **31**, 283 (1973).

8) T. Fueno, V. Bonačić-Koutecký, and J. Koutecký, *J. Am. Chem. Soc.*, **105**, 5547 (1983).

9) T. Fueno, O. Kajimoto, and V. Bonačić-Koutecký, *J. Am. Chem. Soc.*, **106**, 406 (1984).

10) C. F. Melius and J. S. Binkley, 20th Symp. (Internat.) on Combustion, Combustion Inst., Pittsburgh (1984), p. 575.

11) W. J. Hehre, W. A. Lathan, M. D. Newton, R. Ditchfield, and J. A. Pople, QCPE Program No. 236, Indiana Univ., Bloomington, Ind.

12) R. Ditchfield, W. J. Hehre, and J. A. Pople, *J. Chem. Phys.*, **54**, 724 (1971).

13) R. J. Buenker, and S. D. Peyerimhoff, *Theor. Chim. Acta (Berl.)*, **35**, 33 (1974); **39**, 217 (1975).

14) R. J. Buenker, "Studies in Physical and Theoretical Chemistry," R. Carbo, Elsevier, Amsterdam (1982), Vol. 21, pp. 17—34.

15) R. J. Buenker and R. A. Phillips, *J. Mol. Struct. (Theochem)*, **123**, 291 (1985).

16) S. R. Langhoff and E. A. Davidson, *Int. J. Quant. Chem.*, **8**, 61 (1974).

17) R. J. Buenker, *Int. J. Quant. Chem.*, **29**, 435 (1986).

18) P. J. Bruna and S. D. Peyerimhoff, "Ab initio Methods in Quantum Chemistry," ed by K. P. Lawley, Wiley-Interscience, New York (1987), Part 1, pp. 1—97.

19) Incidentally, the C–C bond scission

$$1(^3FE_C) \longrightarrow CH_2(^3B_1) + CH_2{=}NH\ (^1A') \qquad (1d)$$

which is not shown in Scheme 1, has been found to have ΔE_{CI}=109 kJ mol^{-1}. Its TS appears at the C–C distance of 2.266 Å. The barrier height calculated is ΔE_{CI}^{*}=131 kJ mol^{-1}, so that it could be no more important than reactions 1b and 1c.

20) It is meant that the C–C bond scission

$$\underset{3(^3A'')}{CH_3\text{–}CH_2\text{–}N} \longrightarrow CH_3 + CH_2{=}N\ (^2B_2) \qquad (3b)$$

is likely to be energetically more favorable. The transition state located by the SCF routine has a symmetric (C_s) geometry with the C–C distance of 2.300 Å. The barrier height calculated by the MRD-CI method is ΔE_{CI}^{*}=140 kJ mol^{-1}, a value which is significantly smaller than the value

(169 kJ mol^{-1}) obtained for reaction 3a.

21) R. Cvetanović, *Adv. Photochem.*, **1**, 115 (1963).

22) The final states of reactions 1′a and 1′c are both found to be in the trans structure.

23) Aside from the TS for reaction 1′a, geometries optimized by the MC SCF method do not alter appreciably from those determined by the conventional UHF SCF procedure.

24) That the N–H bond scission of **2**(^{1}A′), i.e., reaction 2′c, is energetically more favorable than its other unimolecular reactions

$$\mathbf{2'}\mathbf{t}(^1A') \begin{array}{l} \longrightarrow \mathbf{3'}(^1A') \qquad (2'a) \\ \longrightarrow \mathbf{5t}(^2A') + H \qquad (2'b) \end{array}$$

is apparent from the relative stability of **6**+H (see Scheme 1). The C–C bond scission (not show in Scheme 1)

$$\mathbf{2'}\mathbf{t}(^1A') \longrightarrow CH_3 + CH{=}NH\ (^2A') \tag{2'd}$$

has also proved to be less favorable than reaction 2′c; the calculated bond dissociation energy is $\Delta E_{\mathrm{CI}}=388$ kJ mol^{-1}, which is appreciably greater than 319 kJ mol^{-1} obtained for reaction 2′c (see Table 3).

25) It should be noted that reaction 3′a is not the lowest-barrier unimolecular process possible to singlet ethylnitrene **3′**. It is less favorable than the C–C bond scission

$$\mathbf{3'}(^1A'') \longrightarrow CH_3 + CH_2{=}N\ (^2B_2) \tag{3'b}$$

for which $\Delta E_{\mathrm{CI}}{}^{\ast}$ is calculated to be 46 kJ mol^{-1}. Further, the 1,2 hydrogen migration leading to **2′t**(^{1}A′)

$$\mathbf{3'}(^1A') \longrightarrow \mathbf{2'}\mathbf{t}(^1A') \tag{3'c}$$

which is the reverse process of reaction 2′a is by far more advantageous; the calculated barrier height is $\Delta E_{\mathrm{CI}}{}^{\ast}=12$ kJ mol^{-1} (see Table 3). Geometry of the TS (TS5) obtained by the MC SCF procedure is shown in Fig. 6. Other patterns of unimolecular reactions of **3′** including the intramolecular insertion giving **7** were dealt with elsewhere.[26]

26) T. Fueno, *J. Mol. Struct. (Theochem)*, **170**, 143 (1988).

27) H. Bock and R. Dammel, *Angew. Chem., Int. Ed. Engl.*, **26**, 504, (1987), and the references cited therein.

28) H. F. Hunziker, H. Knappe, and H. R. Wendt, *J. Photochem.*, **17**, 377, (1981).

29) Y. Endo, S. Tsuchiya, C. Yamada, E. Hirota, and S. Koda, *J. Chem. Phys.*, **85**, 4446 (1986).

30) T. Fueno, K. Yamaguchi, and Y. Takahara, *Chem. Phys. Lett.*, in press.

31) P. C. Hariharan and J. A. Pople, *Theor. Chim. Acta (Berl.)*, **28**, 213 (1973).

32) S. W. Benson, "Thermochemical Kinetics," 2nd ed, Wiley, New York (1976).

33) The experimental heat of formation, $\Delta H^\circ_{\mathrm{f0}}=3.65\pm0.10$ eV, for NH($^3\Sigma^-$) has been taken from L. G. Piper, *J. Chem. Phys.*, **52**, 1303 (1980).